Preparation and Optical Performance of Chiral Polymers Having Azobenzene Segments

Jui-Hsiang Liu, Po-Chih Yang

Department of Chemical Engineering, National Cheng Kung University, Tainan 70101, Taiwan, Republic of China

Received 18 August 2003; accepted 3 October 2003

ABSTRACT: A series of monomeric azobenzene derivatives of 6-(4-nitro-4′-oxy-azobenzene acrylate with carbon numbers of 6 and 11, and the chiral monomer of bornyl 4-(6-acryloyloxyhexyloxy)-phenyl-4′-benzoate were synthesized. Chiral polymers having bornyl group end-capped pendants with azobenzene-derived segments were prepared. Molecular structures and polymer compositions were confirmed by using ^{1}H-NMR, elemental analysis, FTIR, and UV–vis analyzers. Thermodynamic properties of both monomers and polymers were investigated. Specific rotations of chiral monomers and polymers were estimated by using an automatic digital polarimeter. Liquid crystalline textures of monomers and polymers were analyzed by using a polarizing optical microscope and confirmed by a small-angle X-ray analyzer. The optical reflection characteristics of composite cells with chiral nematic liquid crystal and various amounts of azobenzene derivatives were evaluated by using a UV–vis spectrophotometer. The reliability and stability of the composite cells with E48/S811 and azobenzene derivatives were studied. The photoisomerization of the chiral polymer film was investigated by using SEM and AFM analyzers. It was found that the UV irradiation of a laser spot caused the shrinkage of polymer film due to the photoisomerization of azobenzene segments. The contraction of the polymer film can be recovered by heat treatment.
© 2004 Wiley Periodicals, Inc. J Appl Polym Sci 91: 3693–3704, 2004

Key words: chiral; photochemistry; atomic force microscopy (AFM); UV–vis spectroscopy; optical properties

INTRODUCTION

Liquid crystalline polymers containing azo groups on the side chain were recently proposed as materials for optical storage.[1] Optical properties of polymer films that can be varied selectively and reversibly by light have considerable potential for use in photonics.[2–4] Azobenzene derivatives as photochromic liquid crystals have been explored as photonic materials because they can change not only their own optical properties but the optical anisotropy of the surrounding liquid crystal molecules by photoirradiation.[5] *trans–cis* Photoisomerization of the azobenzene molecules in the liquid crystal phase can disorganize the phase structure of liquid crystal molecules, resulting in liquid crystal to isotropic isothermal phase transition.[6,7] The photochemical phase transition of liquid crystals has been examined conveniently by transmission and reflection mode analyses.[8–12]

Two structural factors receive special attention because they allow control over the levels and rates of induced birefringence. The first factor is the thermodynamic tendency of the polymer to form organized domains. If the polymer is crystalline or liquid crystalline, the photoinduced supramolecular organization is reinforced and the levels of birefringence attainable in such systems are significantly higher than those in amorphous polymer films. The disadvantage of the crystalline/liquid crystalline materials, however, is that it takes much longer to induce the birefringence, given that the process involves complex motions to form whole crystalline/liquid crystalline domains. Also, it is difficult and time-consuming to "erase" because randomness is never restored; only the directionality of various crystalline domains is randomized.

The second factor is the existence of cooperative motions of the neighboring groups, which may enhance the orientation. This factor is well known in crystalline and liquid crystalline materials. In liquid crystalline polymer films containing azo and ester/amide mesogens,[13] changing the direction of the azo mesogens using polarized light will activate the photoinactive mesogens to move in concert, thus recreating the initial liquid crystalline order. A similar phenomenon was previously described in azo-containing Langmuir–Blodgett films,[14] where liquid crystals can change their orientation by sympathy with the *trans–cis* isomerization of the adjacent azobenzenes.

From such a viewpoint, the light-scattering mode control of light was proposed and accomplished by using a polymer matrix combined with the liquid crystal system in lieu of the function of the polarizers similar to a polymer dispersed liquid crystal

Correspondence to: J.-H. Liu (jhliu@mail.ncku.edu.tw).

Journal of Applied Polymer Science, Vol. 91, 3693–3704 (2004)
© 2004 Wiley Periodicals, Inc.

(PDLC).[15–18] In general, the light-scattering state is operated through electrical control of the ordering of the liquid crystal domains as in other liquid crystal devices. PDLCs with a memory function, which have potential for image storage and laser addressed displays, were also reported.[19–22] In these composite films, optical information can be recorded because of a reversible change in threshold frequency induced by the isomerization of azobenzene.

In our previous study, we reported optical control of the light through the polymer/liquid crystal composite film based on the control of the electric field.[23–25] In the systems, phase separation of polymers in liquid crystal leads to the formation of focal–conic texture domains. In the case of an absence of an electric field, the focal–conic structure is formed and caused by the light-scattering phenomena. When an electric field is applied to the polymer stabilized cholesteric texture (PSCT) cells, the director of liquid crystals reorients parallel to the direction of the applied field and the PSCT cells become transparent.

In this study, a series of monomeric azobenzene derivatives of 6-(4-nitro-4′-oxy-azobenzene acrylate with carbon numbers of 6 and 11, and the chiral monomer of bornyl 4-(6-acryloyloxyhexyloxy)phenyl-4′-benzoate were synthesized. Polymerization of the azobenzene-derived monomers and chiral monomers was carried out. The thermostability, anisotropic texture, and optical properties of the polymers were investigated. Photoisomerization of polymer films was also investigated by using SEM and atomic force microscopy (AFM).

EXPERIMENTAL

Measurements

FTIR spectra were recorded on a Jasco VALOR III (Tokyo, Japan) FTIR spectrophotometer. Nuclear magnetic resonance (NMR) spectra were obtained on a Bruker AMX-400 (Darmstadt, Germany) high-resolution NMR spectrometer. Optical rotations were measured at 30°C in dimethylformamide (DMF) using a Jasco DIP-360 automatic digital polarimeter with readings to ±0.001°. Elemental analyses were conducted with a Heraeus CHN-O (Darmstadt, Germany) rapid elemental analyzer. Gel permeation chromatography (GPC) measurements were carried out at 40°C on a Hitachi L-4200 (Osaka, Japan) instrument equipped with TSK gel GMH and G2000H columns using THF as an eluent. Thermal analyses of the azobenzene compounds and PDLC films were performed by differential scanning calorimeter (DSC; Perkin Elmer Cetus Instruments, Norwalk, CT) at a heating and cooling rate of 10 K/min in nitrogen atmosphere. The liquid crystal phases were investigated by an Olympus BH-2 (Osaka, Japan) polarized optical microscope (POM) equipped with Mettler hot stage (Model FP-82; Greifensee, Switzerland) and the temperature scanning rate was determined at a rate of 5 K/min. SEM microphotographs were measured with a JEOL JSM-35 (Osaka, Japan) instrument; AFM microphotographs were recorded on a Digital Instruments (Santa Barbara, CA) Nanoscope III analyzer DI NS3a-2/MMAFM.

Materials

Nematic liquid crystal mixture E48 and chiral liquid crystal S811 were purchased from Merck (Darmstadt, Germany). Monomers used in this investigation were all synthesized as follows. The products were all identified by using spectrophotometers.

4-(6-Hydroxyhexyloxy) benzoic acid (1a)

4-Hydroxybenzoic acid (16.57 g, 120 mmol) was dissolved in a mixture of EtOH (42 mL) and H_2O (18 mL). KOH (17.8 g. 317.8 mmol) and a catalytic amount of KI dissolved in EtOH (50 mL) were added dropwise to the solution. 1-Chloro-6-hexaol (22.5 g, 165 mmol) was then added, and the solution was heated to reflux for 24 h. The resulting mixture was poured into water and extracted with ethyl ether. The water phase solution was acidified with HCl diluted with water until weakly acidic. The resulting precipitate was filtered and washed several times with water. The crude product was recrystallized from EtOH/H_2O (4/1). Yield: 19.1 g (67%), T_m = 139–140°C.

FTIR (cm^{-1}): 3249 (OH), 1685(C═O), 1287, 1251 (C—O—C). ^{1}H-NMR, DMSO-d_6, δ (ppm): 12.6 (s, 1H, –COOH), 7.9 (d, 2H Ar, *ortho* to –COOH), 7.0 (d, 2 H, Ar, *meta* to –COOH), 4.4 (s, 1H, OH), 4.0 (t, 2H, –CH_2OPh–), 3.4 (t, 2H, –CH_2—OH), 1.28–1.74 (m, 8H).

4-(11-Hydroxyundecandecyloxy) benzoic acid (1b)

Compound 1b was similarly synthesized. Yield: 54.7%; K 111°C N 148°C I.

4-(6-Acryloyloxyhexyloxy) benzoic acid (2a)

Compound 1a (7.15 g, 31.5 mmol), *N*,*N*-dimethylaniline (4 g, 33.0 mmol), and a catalytic amount of 2,6-di-*tert*-butyl-*p*-cresol were dissolved in distilled 1,4-dioxane (50 mL). The solution was cooled with an ice/salt bath and then acryloyl chloride (9 mL, 99.3 mmol) dissolved in distilled 1,4-dioxane (20 mL) was added dropwise under vigorous stirring. After completing a 24-h reaction at room temperature, the solution was poured into cold water and the precipitate was filtered. The crude product was washed several times with water and recrystallized twice from EtOH. Yield: 6.3 g (69%); K 88°C N 92°C I.

FTIR (cm^{-1}): 2945, 2864 (CH_2), 1725 (C═O), 1604, 1291, 1246 (C—O—C), 1675 (C═C). ^{1}H-NMR, $CDCl_3$, δ (ppm): 12.5 (s, 1H, –COOH), 8.0 (d, 2H, Ar, *ortho* to –COOH), 7.0 (d, 2H, Ar, *meta* to –COOH), 5.8, 6.4, 6.1 (s, 3H, H_2C═CH–), 4.1 (t, 2H, –$COOCH_2$–), 4.0 (t, 2H, –CH_2OPh–), 0.94–1.28 (m, 8H, –CH_2–).

4-(11-Acryloyloxyundecyloxy) benzoic acid (2b)

Compound 2b was similarly synthesized. Yield: 79%; K 99°C N 108°C I.

4-Hexyloxyphenyl-4′-(6-acryloyloxyhexyloxy) benzoate (3a)

Compound 2a (2.92 g, 10.0 mmol) and 4-hexyloxyphenol (2.91 g, 15 mmol) were dissolved in CH_2Cl_2 (40 mL) at 30°C. *N,N′*-Dicyclo-hexylcarbodiimide (DCC) (3.09 g, 15.0 mmol) and *N,N′*-dimethyl-aminopyridine (DMAP) (0.1 g, 0.82 mmol) were dissolved in CH_2Cl_2 (30 mL), and the mixture was then added to the former solution. The mixture was stirred for 2 days at 30°C. The resulting solution was filtered and washed with water, dried with $MgSO_4$, and evaporated. The crude product was purified by column chromatography with silica gel using ethyl acetate/*n*-hexane = 1/4 as eluate and recrystallized twice from EtOH. Yield: 2.76 g (59%); K 57°C N 62°C I.

FTIR (cm^{-1}): 2933, 2865 (CH_2), 1725 (C═O), 1635 (C═C). ^{1}H-NMR, acetone-d_6, δ (ppm): 8.1 (d, 2 aromatic H, *ortho* to –COOPh–), 7.1 (d, 2 aromatic H, *meta* to –OC_6H_{13}), 7.0 (d, 2 aromatic H, *meta* to –COOPh–), 6.9 (d, 2 aromatic H, *ortho* to –OC_6H_{13}), 6.3, 6.2, 5.9 (s, 3H, H_2C═CH–), 4.1 (t, 2H, –$COOCH_2$–), 4.0 (t, 2H, –CH_2OPh–), 1.26–1.42 (m, 8H, –CH_2–), 0.86–0.91 (m, 13H, –OC_6H_{13}).

ANAL. calcd for $C_{28}H_{36}O_6$: C, 71.80%; H, 7.70%. Found: C, 71.78%; H, 7.82%.

The following compounds were synthesized by using methods similar to those described above and are all identified.

4-Nitrophenyl-4′-(11-acryloyloxyhexyloxy) benzoate (3a′)

Yield: 60.1%; K 75.9°C I.

ANAL. calcd for $C_{22}H_{23}NO_7$: C, 63.92%; H, 5.57%; N, 3.40%. Found: C, 63.89%; H, 5.68%; N, 3.49%.

4-Hexyloxyphenyl-4′-(6-acryloyloxyundecyloxy) benzoate (3b)

Yield: 65.1%; K 52°C N 65°C I.

ANAL. calcd for $C_{33}H_{46}O_6$: C, 73.63%; H, 8.55%. Found: C, 73.62%; H, 8.58%.

4-Nitrophenyl-4′-(6-acryloyloxyundecyloxy) benzoate (3b′)

Yield: 70.4%; K 87.4°C I.

ANAL. calcd for $C_{27}H_{33}NO_7$: C, 67.08%. H, 6.83%; N, 2.90%. Found: C, 67.04%;, H, 6.92%; N, 2.98%.

4-Hydroxy-4′-nitro-azobenzene (4)

4-Nitroaniline (5 g, 36.23 mmol) was dissolved in 1*M* aqueous HCl (100 mL) and kept in the ice bath at 0°C. $NaNO_2$ (3.53 g, 51.16 mmol) in water (20 mL) was added dropwise to the former solution and stirred for 30 min. NaOH (4.4 g, 0.11 mol) and phenol (5.0 g, 53.19 mmol) were dissolved in water (100 mL) and stirred for 30 min at 0°C. The former solution was added dropwise to the latter solution at 0°C and then stirred for 1 h. The resulting mixture was poured into water and the solution was neutralized with 5% aqueous HCl. The crude product was filtered and recrystallized twice from EtOH. Yield: 6.0 g (68.1%), red crystalline powder; T_m = 220°C.

FTIR (cm^{-1}): 3450 (OH), 1510 (NO_2). ^{1}H-NMR, $CDCl_3$, δ (ppm): 7.9–8.0 (d, 4 aromatic H, Ar—N═*N*—Ar–), 8.3 (d, 2 aromatic H, *ortho* to NO_2), 7.0 (d, 2 aromatic H, *ortho* to OH), 5.6 (s, 1H, –OH).

1-Hydroxy-*n*-(4-nitro-azobenzene-4′oxy)hexane (5a)

Compound 4 (4.0 g, 16.50 mmol) was dissolved in *N,N*-dimethylacetamide (150 mL). KOH (1.1 g, 19.8 mmol), dissolved in *N,N*-dimethyl acetamide (30 mL), was added dropwise to the former solution; 1-chloro-6-hexanol (14.5 g, 103.9 mmol) and a trace of KI were than added, and the solution was heated at reflux for 30 h. The resulting mixture was poured into water and extracted with CH_2Cl_2. After drying, the crude product was recrystallized twice from EtOH. Yield: 3.22 g (57%); K 112°C N 125°C I (cooling).

FTIR (cm^{-1}): 3557 (OH), 2940, 2864 (CH_2), 1706 (CO in Ar—COO–), 1600, 1501 (C—C in Ar), 1260 (COC), 1510(NO_2). ^{1}H-NMR, $CDCl_3$, δ (ppm): 8.3 (d, 2 aromatic H, *ortho* to NO_2), 8.0 (d, 4 aromatic H, Ar—N═*N*—Ar–), 7.0 (d, 2 aromatic H, *ortho* to –O–), 5.5 (s, 1H, –OH), 4.1 (t, 2H, –CH_2OPh–), 3.7 (2H, *ortho* to OH), 0.94–1.28 (m, 8H, –CH_2–).

1-Hydroxy-*n*-(4-nitro-azobenzene-4′-oxy)undecane (5b)

Compound 5b was similarly synthesized. Yield: 67%; K 93°C N 112°C I.

6-(4-Nitro-4′-oxy-azobenzene) alkyl acrylate (6a)

Compound 5a (2.0 g, 5.83 mmol), *N,N*-dimethylaniline (2.0 g, 16.5 mmol), and a catalytic amount of 2,6-di-*tert*-butyl-*p*-cresol were dissolved in distilled 1,4-diox-

TABLE I
Thermodynamic Properties of Compounds Synthesized in Schemes 1 and 2

Compound	Heating cycle (°C)[a]	Cooling cycle (°C)	ΔH_{NI} (J/g)
1a	K 140 I	—	—
1b	K 111 N 148 I	K 101 S_A 125 N 132 I	6.85 (−3.05[b])
2a	K 88 N 92 I	—	13.01
2b	K 99 N 108 I	—	2.14
3a	K 57 N 62	—	0.07
3a′	K 75.9 I	K 60.8 I	—
3b	K 52 N 65 I	—	8.76
3b′	K 87.4 I	K 67.8 I	—
4	K 220 I	—	—
5a	—	K 112 N 125 I	1.11
5b	K 93 N 112 I	K 70 N 106 I	7.32 (−6.91)
6a	K102 I	K 68 I	—
6b	K94 I	K 73 I	—

[a] K, crystal; S_A, smectic A; N, nematic; I, isotropic.
[b] Enthalpy during cooling.

ane (30 mL). The solution was cooled with an ice/salt bath and then acryloyl chloride (1.05 g, 11.7 mmol), dissolved in distilled 1,4-dioxane (20 mL), was added dropwise under vigorous stirring. The mixture was stirred for 8 h at room temperature. After completing the reaction, the solution was poured into cold water and the precipitate was filtered. The crude product was washed several times with water and recrystallized twice from EtOH. Yield: 1.9 g (82%); T_m = 102°C.

FTIR (cm^{-1}): 2940, 2864 (CH_2), 1687 (C═C), 1510 (NO_2). ^{1}H-NMR, $CDCl_3$, δ (ppm): 8.3 (d, 2 aromatic H, *ortho* to NO_2), 8.0 (d, 4 aromatic H, Ar—N═*N*—Ar–), 7.0 (d, 2 aromatic H, *ortho* to –O–), 5.8, 6.1, 6.4 (s, 3H, H_2C═CH–), 3.8–4.1, 0.94–1.28 (m, 12H, $–CH_2–$). From the UV–vis spectrum, λ_{max} = 386 nm ($CHCl_3$).

ANAL. calcd for $C_{21}H_{23}N_3O_5$: C, 63.50%; H, 5.80%; N, 10.60%. Found: C, 63.24%; H, 5.94%; N, 10.69%.

6-(4-Nitro-4′-oxy-azobenzene) undecyl acrylate (6b)

Compound 6b was similarly synthesized. Yield: 83%; T_m = 94°C. From the UV–vis spectrum, λ_{max} = 386 nm ($CHCl_3$).
ANAL. calcd for $C_{26}H_{33}N_3O_5$: C, 66.81%; H, 7.07%; N, 9.00%. Found: C, 66.56%; H, 7.14%; N, 9.08%.

Bornyl 4-(6-acryloyloxyhexyloxy) phenyl-4′-benzoate (7)

Compound 2a (8.5 g, 29.1 mmol) and bornyl 4-hydroxybenzoate (7.9 g, 29.0 mmol) were dissolved in

TABLE II
Results of Polymerization and Phase-Transition Temperatures of Polymers

	Composition				Phase-transition temperature (°C)						
Polymer	$x/y/z$[a]	$x/y/z$[b]	m/n[c]	R[d]	Heating	Cooling	M_w	M_w/M_n	Yield (%)	ΔH_{SI} (J/g)	$[\alpha]_D^{25}$[e]
P1	0/0/100	0/0/100	—/6	OC_6H_{13}	G 115.0 I	G 108.5 I	33400	1.28	65	—	—
P2	0/0/100	0/0/100	—/11	OC_6H_{13}	G 66.4 S_A 116.4 I	G 60.8 S_A 112.0 I	30050	1.22	70	9.45	—
P3	7/0/93	8.2/0/91.8	6/6	OC_6H_{13}	G 105.9 I	G 103.0 I	14250	1.42	63	—	—
P4	7/0/93	8.0/0/92.0	11/6	OC_6H_{13}	G 105.7 I	G 103.5 I	16060	1.50	64	—	—
P5	7/0/93	8.2/0/91.8	6/11	OC_6H_{13}	G 56.4 S_A 113.2 I	G 51.6 S_A 108.1 I	12440	1.37	65	7.74	—
P6	7/0/93	7.9/0/92.1	11/11	OC_6H_{13}	G 61.2 S_A 118.4 I	G 56.4 S_A 111.8 I	16730	1.43	60	6.94	—
P7	7/10/83	7.9/8.1/84.0	6/6	OC_6H_{13}	G 96.0 I	G 95.6 I	11220	1.41	45	—	−4.4
P8	7/10/83	7.7/7.5/84.8	11/6	OC_6H_{13}	G 95.7 I	G 95.1 I	11040	1.39	42	—	−6.8
P9[f]	7/10/83	7.5/7.6/84.9	6/11	OC_6H_{13}	G 40.7 S* 99.7 I	G 35.3 S* 98.0 I	11220	1.38	44	5.81	−9.2
P10[g]	7/10/83	10.3/5.8/83.9	11/11	OC_6H_{13}	G 45.0 S* 103.0 I	G 39.8 S* 98.5 I	11460	1.43	41	3.45	−8.1
P11	7/0/93	8.6/0/91.4	6/6	NO_2	G 89.9 I	G 88.9 I	12060	1.31	58	—	—
P12	7/0/93	7.9/0/92.1	11/6	NO_2	G 90.7 I	G 88.6 I	11920	1.75	55	—	—
P13	7/0/93	5.0/0/95.0	6/11	NO_2	G 92.7 I	G 90.1 I	9460	1.47	54	—	—
P14	7/0/93	5.1/0/94.9	11/11	NO_2	G 104.7 I	G 100.6 I	8940	1.50	52	—	—

[a] Feed molar ratio of monomers.
[b] Molar ratio of polymers from elemental analysis.
[c] Alkyl length of monomers.
[d] Terminal substituents of compounds.
[e] Specific rotation of polymers, 0.1 g in 10 mL THF.
[f] Layer thickness of smectic calculated from X-ray diffraction, d = 30.5 Å.
[g] Layer thickness of smectic calculated from X-ray diffraction, d = 36.5 Å.

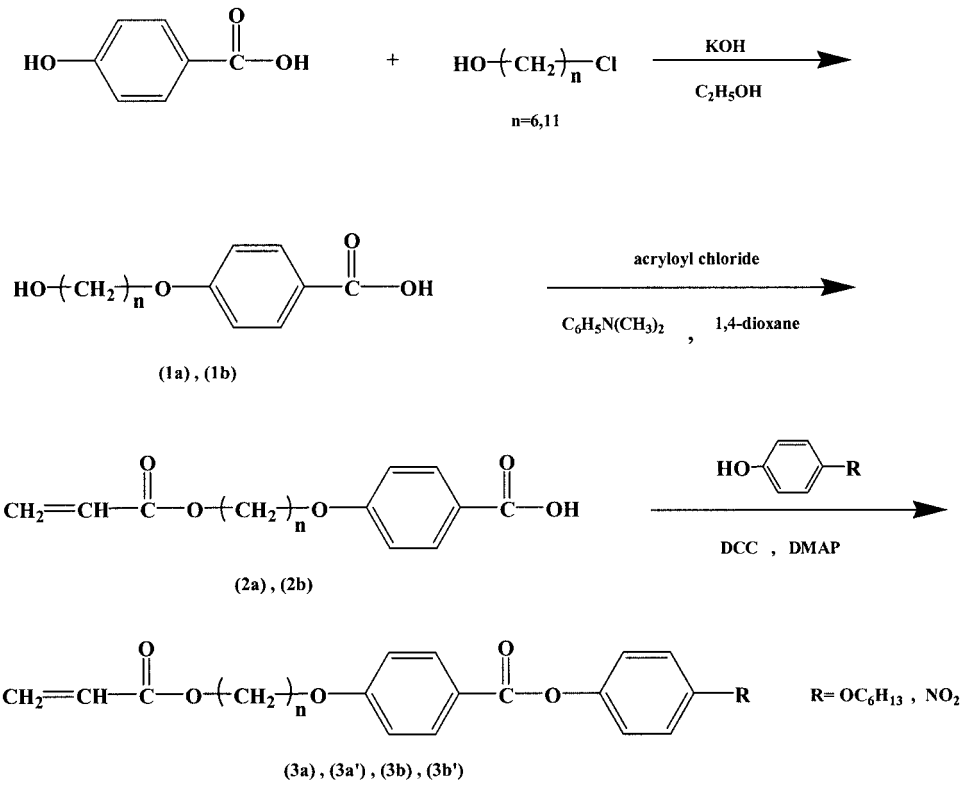

Compound	n	R
3a	6	OC_6H_{13}
3a'	6	NO_2
3b	11	OC_6H_{13}
3b'	11	NO_2

Scheme 1

CH_2Cl_2 (100 mL) at 30°C. DCC (18.0 g, 87.0 mmol) and DMAP (0.34 g, 2.9 mmol) were dissolved in CH_2Cl_2 (50 mL), then added to the former solution, and stirred for 2.5 days at 30°C. The resulting solution was filtered and washed with water, dried over $MgSO_4$, and then evaporated. The crude product was purified by column chromatography (silica gel, ethyl acetate/hexane, 1/8) and recrystallized twice from EtOH. Yield: 6.1 g (39%); T_m = 55–56°C. (The equation and the molecular structures are shown below in Scheme 3.)

IR (cm^{-1}): 2945, 2873 (CH_2), 1741 (CO in Ar—COO–), 1608, 1505 (C—C in Ar), 1198, 1244 (COC), 1710 (CO in Ar—COO—Ar′), 1633 (C═C). ^{1}H-NMR, $CDCl_3$, δ (ppm): 0.93–2.49 (m, 24H), 4.06 (m, 2H), 4.19 (m, 2H), 5.13 (m, 1H), 5.82 (m, 1H), 6.14 (m, 1H), 6.43 (m, 1H), 6.99 (d, 2H), 7.28 (d, 4H), 8.15 (d, 4H).

LC cell preparation

The liquid crystal composite cells were prepared from the mixture of E48/S81/azobenzene derivatives. Because E48 is a kind of nematic liquid crystal mixture, the composition is too complex. For convenience, the weight ratio of E48/S811/Azo = 0.2/0.06/0.002–0.006 g was used. The mixture was treated ultrasonically to form a homogeneous solution, and then injected into a glass cell separated with a 15-μm spacer.

Polymerization

The homopolymers and copolymers were prepared by radical polymerization in a sealed ampoule with 3 mol % of AIBN in anhydrous benzene at 60°C for 24 h. The polymer was purified by repeated precipitation with methanol and dried in vacuum. The results and the

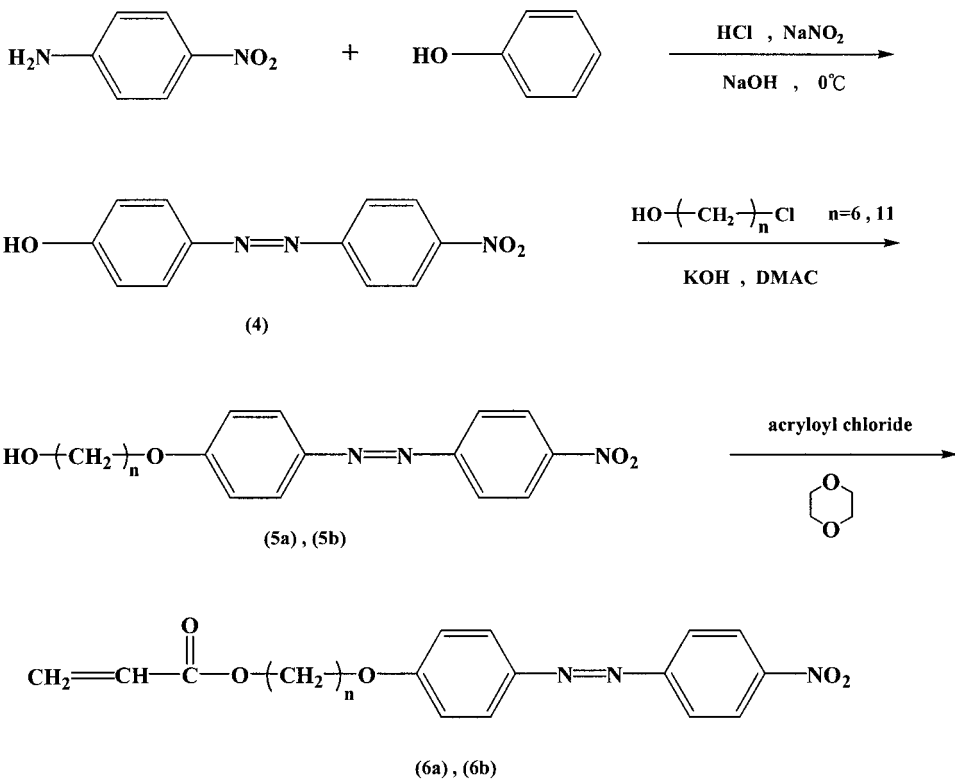

Compound	n
6a	6
6b	11

Scheme 2

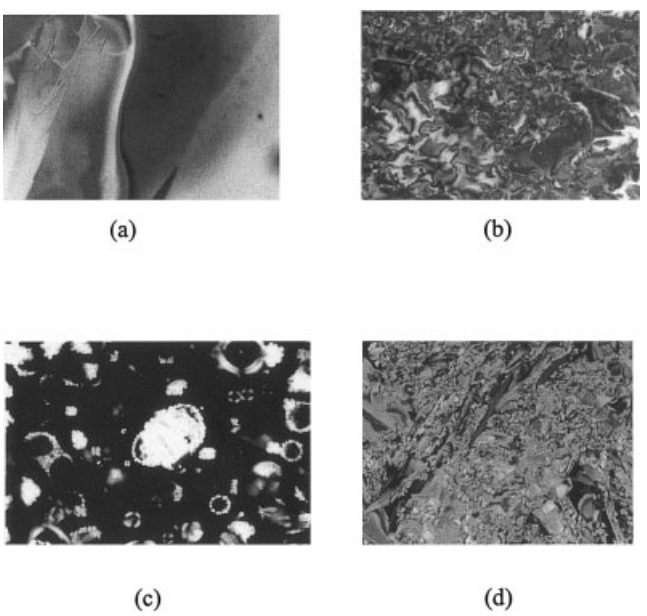

Figure 1 POM textures of compounds: (a) 2a; (b) 2b; (c) 3b; (d) 5a.

physical properties of the polymers are shown in Tables I and II.

RESULTS AND DISCUSSION

Scheme 1 shows the synthetic process of a series of monomers derived from 4-hydroxybenzoic acid. An electron-releasing OC_6H_{13} and an electron-withdrawing NO_2 were introduced onto the terminal of the molecules. To study the spacer effects on the molecules, C_6H_{12} and $C_{11}H_{22}$ spacers with different carbon lengths were introduced between the pendant group and acrylic double bond. As shown in Scheme 1, four kinds of acrylic monomers with various lengths and terminal groups were synthesized. The molecular structures were confirmed by ^{1}H-NMR, elemental analysis, and FTIR analyzers.

Scheme 2 shows the synthetic process of azobenzene monomers having C_6 and C_{11} spacers with a terminal electron-withdrawing NO_2. Two kinds of azobenzene derivatives with different carbon lengths were synthesized. The thermodynamic properties of azobenzene derivatives are summarized in Table I. As

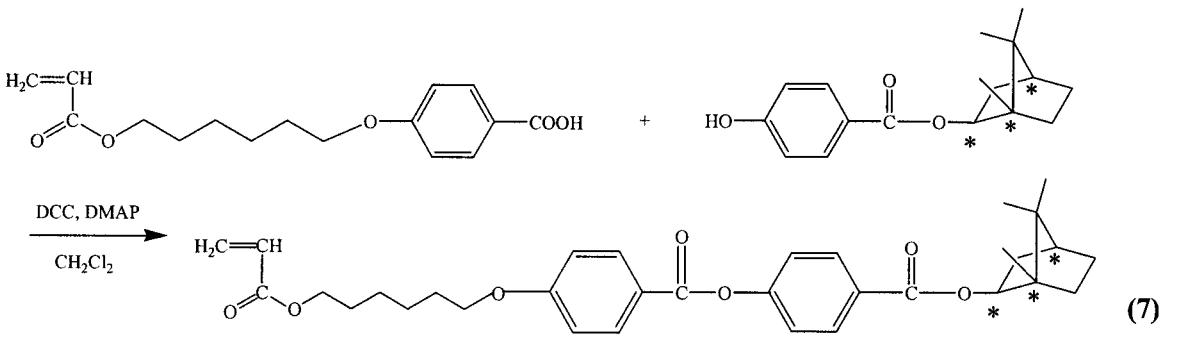

Scheme 3

can be seen in Table I, some of the esters and the azobenzene derivatives showed liquid crystalline phases on their heating and cooling cycles. The enthalpy (ΔH) required for phase change from nematic (N) to isotropic (I) was also estimated. For compound **1b**, different ΔH values on heating and cooling cycles were observed. The result shows that molecular arrangement and the strength of the intermolecular forces between liquid crystal molecules are different during the cycles. The results can also be seen in DSC phase change analyses as shown in Table I, K 111 N 148 I for the heating cycle and K 101 S_A 125 N 132 I for the cooling cycle.

Phase-transition temperatures were estimated by using a differential scanning calorimeter (DSC). Isotropic and liquid crystalline phases were confirmed by a polarizing optical microscopic (POM) analyzer. Figure 1 shows some examples of liquid crystalline optical textures of compounds. The liquid crystalline phases were analyzed by a POM analyzer and then determined by comparing the optical textures of compounds with those described in the literature. The liquid crystalline phases were also identified by using a small-angle X-ray diffraction analyzer.

To study the optical properties of chiral polymers having azobenzene pendant groups, a series of polymers were synthesized. Scheme 3 and Scheme 4 show the synthesis of chiral monomers and the structure of the copolymers prepared in this study, respectively. The results of the polymerization are summarized in Table II. Molar ratios of polymers were evaluated by elemental analyses. The specific rotation of chiral polymers having bornyl groups was estimated. All chiral polymers revealed a left rotation. The chirality of the chiral polymers can be expected to affect the arrangement and the helical pitch of chiral liquid crystals while they are added in liquid crystals as dopants. As can be seen in Table II, only molecules having $n = 11$ spacers revealed liquid crystalline phases. The thickness of the layers of the smectic phase was estimated by using a small-angle X-ray diffraction analyzer. It was found that the temperature paths of the heating and cooling cycles are different. The results show that the liquid crystals synthesized in Table II are monotropic liquid crystals. The molecular arrangement and the strength of the intermolecular forces may be different during the cycles. The S* symbol in Table II indicates the chiral smectic phase. In theory,

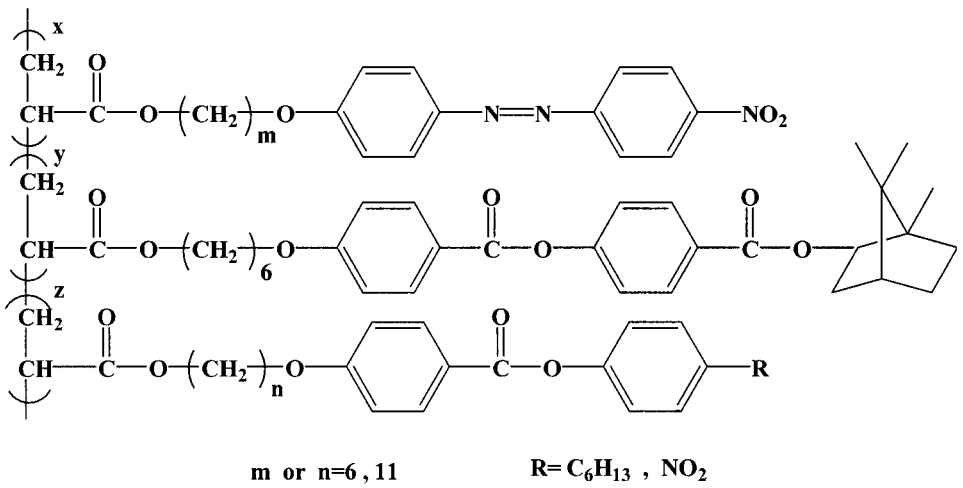

Scheme 4

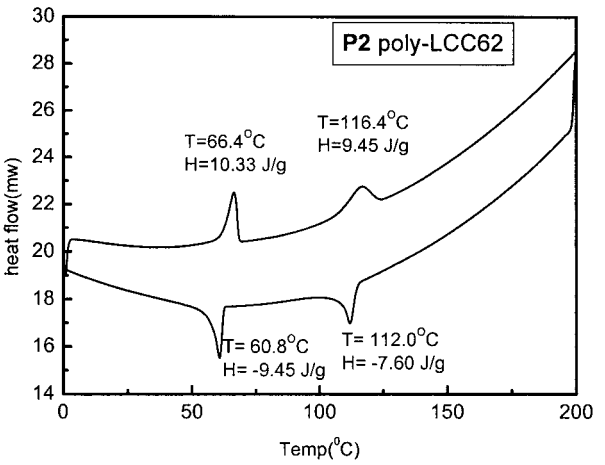

(a)

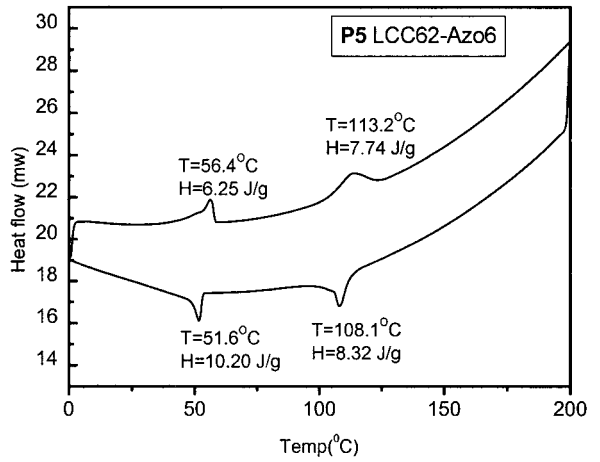

(b)

Figure 2 DSC curves of P2 and P5.

the director of S* molecules will rotate along an axis because of the existence of the chiral units. Figures 2 and 3 show the DSC curves and optical textures of polymers synthesized in this study, respectively. The monotropic characteristics and the smectic optical textures of the liquid crystals can all be seen in the figures.

The thermal resistance of polymers was evaluated by using a thermal gravimetric analyzer (TGA). The results are summarized in Table III. Both homopolyesters P1 and P2 revealed a good initial thermal resistance, which may be attributable to the absence of NO_2 and bornyl groups in the side chain. It was found that

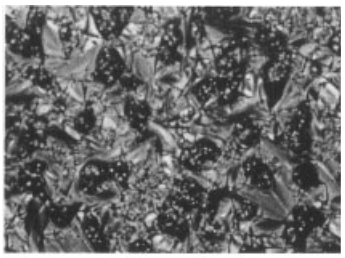

(a)

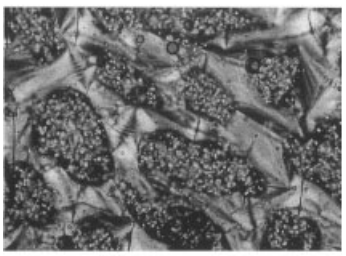

(b)

Figure 3 POM textures of (a) P2 and (b) P5 at 80°C.

high steric hindered bornyl groups may increase the glass-transition temperature (T_g) of polymers but not the degradation temperature (T_d).[26,27] As can be seen in Table III, the existence of NO_2 in pendant groups of P11 and P14 may easily cause an initial thermal degradation from the site. However, the further thermal crosslinking from the active sites may also occur, leading to the high thermal resistance of the polymers at 600°C.

To investigate the photoinduced selective reflection of chiral nematic liquid crystal cells, a series of liquid

TABLE III
Thermal Resistance of Polymers

Polymer	Weight loss (°C) 5%	Weight loss (°C) 50%	Residue (wt %) 600°C
P1	404.5	457.5	5.3
P2	400.7	458.6	3.3
P3	385.2	455.9	7.3
P4	382.1	455.5	7.7
P5	383.4	450.8	7.0
P6	389.9	458.4	5.9
P7	375.9	442.2	8.0
P8	369.0	434.9	7.7
P9	380.7	458.0	6.2
P10	379.6	455.9	7.1
P11	335.7	446.7	19.1
P12	339.6	471.6	19.8
P13	346.8	503.1	20.1
P14	349.7	484.0	19.5

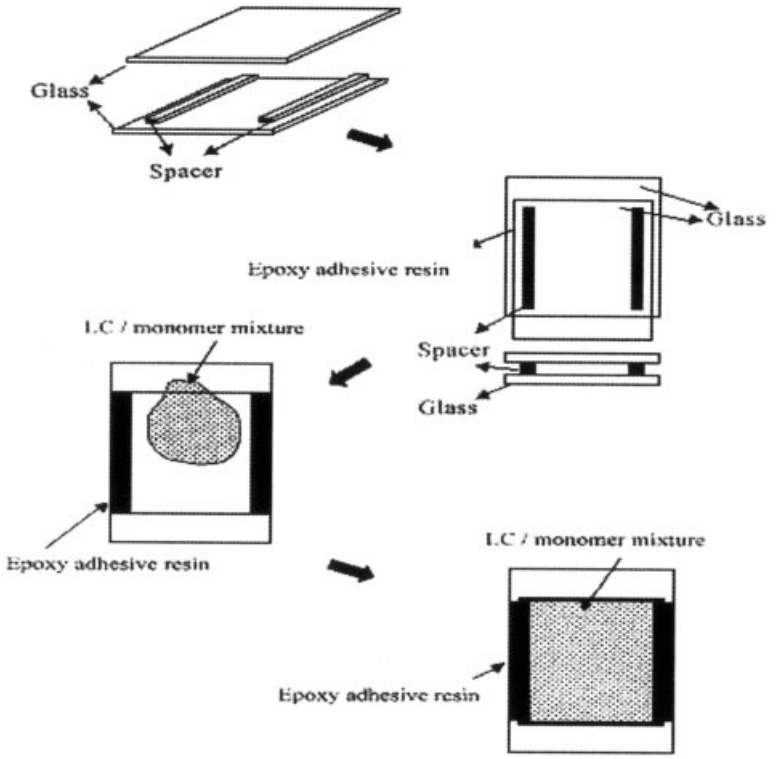

Figure 4 Forming process of liquid crystal cells.

crystal cells with E48/S811 chiral nematic and photosensitive azobenzene derivatives was prepared. Figure 4 shows the forming process of the cells. Figure 5 shows the experimental setup for the investigation of the transmittance and the reflection of the cells prepared in this investigation. Figure 6 shows the results of the dependency of UV–vis spectra of E48/S811 liquid crystal cell on temperature. The reflected wavelength was shifted to the blue side when the temperature was increased. The results may be atributable to the shrinkage of the pitch of the chiral nematic liquid crystal. Effects of the doping amount of the azobenzene derivative 6a on the reflection wavelength are shown in Figure 7. The existence of azobenzene derivatives may cause a shrinkage of pitch, leading to the shift of the reflecting wavelength to the blue side.[28] The expansion of the pitch was found to increase with increasing concentration of azobenzene derivatives. As can be seen in Figure 8, temperature caused the shrinkage of the pitch and shifted the reflecting wavelength to the blue side. For the system, 2 wt % of azobenzene derivative 6a was added as a dopant. The reasons that the wavelength shifted may be the same as those described in Figure 6. The liquid crystal cell

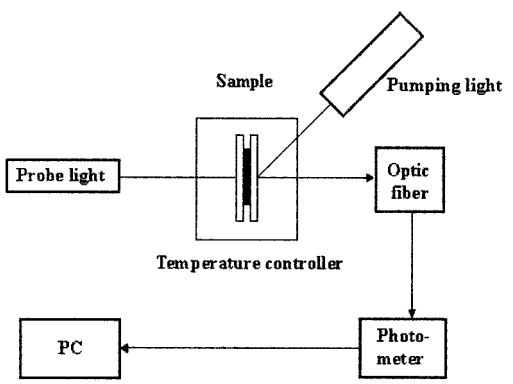

Figure 5 Experimental setup for estimation of transmittance and reflection of composite cells.

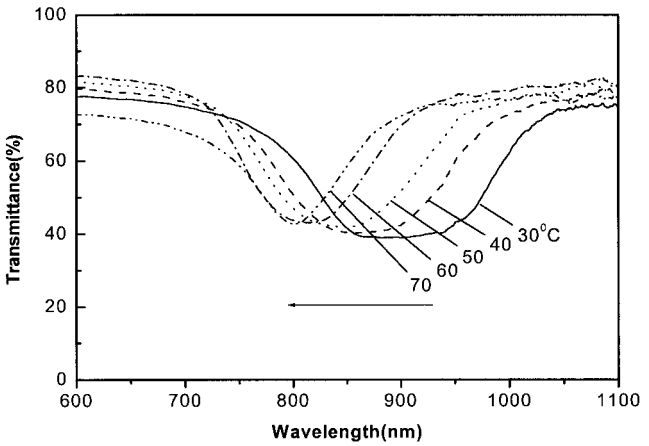

Figure 6 Dependency of UV–vis spectra of E48/S811 liquid crystal cell on temperature.

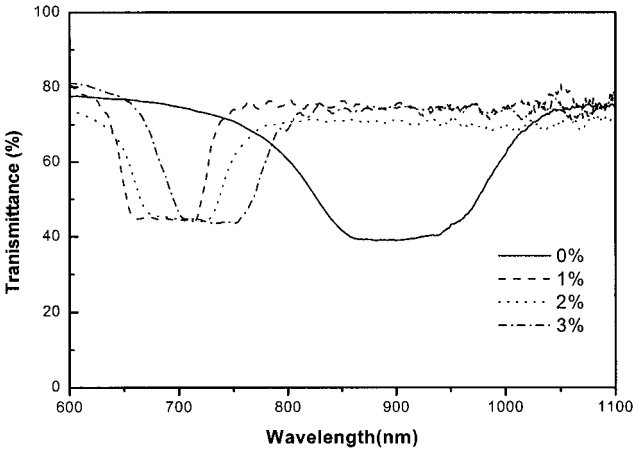

Figure 7 Effects of doping amount of azobenzene derivative **6a** on reflection wavelength.

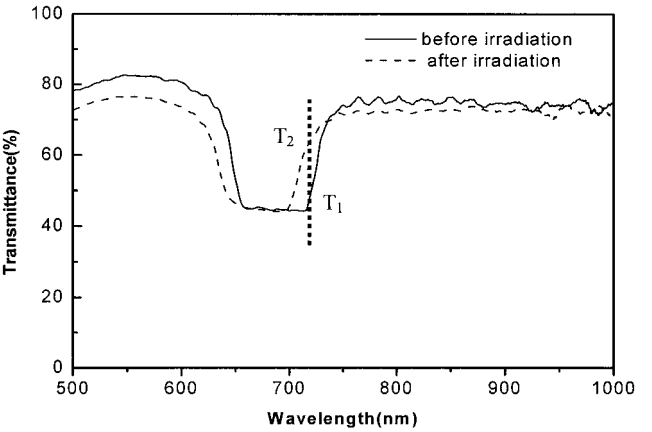

Figure 9 Dependency of reflecting spectra on UV irradiation for E48/S811/1 wt % Azo-6(a) cell.

was changed to isotropic liquid and the optical reflection phenomena can no longer be seen when the cell was heated over 75°C.

Furthermore, to investigate the photoisomerization of azobenzene derivatives and the dependency of the film reflection on UV irradiation, a E48/S811/1 wt % Azo-6(a) composite cell was fabricated and was irradiated with UV light. Figure 9 shows the results of the film transmittance before and after UV irradiation for the E48/S811/1 wt % Azo-6(a) cell (UV source: 0.4 mW; distance: 5 cm; irradiation time: 10 min). The reflected light was shifted to the blue side after UV irradiation, which may be attributable to the photoisomerization of the azobenzene segment from the *trans* to *cis* configuration. In general, a variation of *trans–cis* isomerization will cause a change of helical pitch of the liquid crystal. Besides, variation of electron environments usually causes a shift of UV–vis absorption. As shown in Figure 10, variation of the shift was slightly strengthened as the added **6a** was increased to 3 wt %. The effects of the 6b concentration on the film transmittance are shown in Figure 11. The existence of azobenzene derivatives may also affect the intermolecular action and helical pitch. As compared with those obtained in Figure 7, the variation for 6b revealed a slightly smaller red shift on concentration. The results suggest that a longer spacer C_{11} may strengthen the interaction between 6b and liquid crystal molecules. Thermal effects on the cell reflection were also investigated. As Figure 12 shows, heat treatment caused a blue shift and the liquid crystal phase disappeared when the cell was heated over 75°C. Over this temperature, the chiral nematic liquid crystal mixture may lose its liquid crystalline properties, thus leading to the disappearance of the reflection.

The reliability and the stability of the photoisomerization of the liquid crystal cell with E48/S811/1 wt % Azo-6(a) composition were confirmed. As can be seen in Figure 9, T_1 and T_2 were used as the results of the

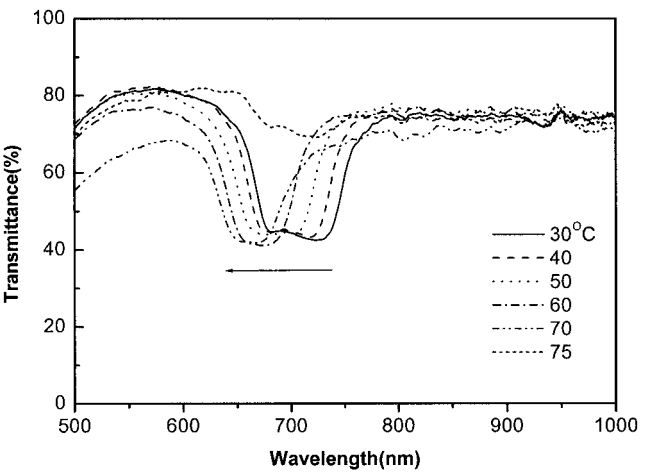

Figure 8 Dependency of reflecting spectra on temperature for E48/S811/2 wt % Azo-6(a) cell.

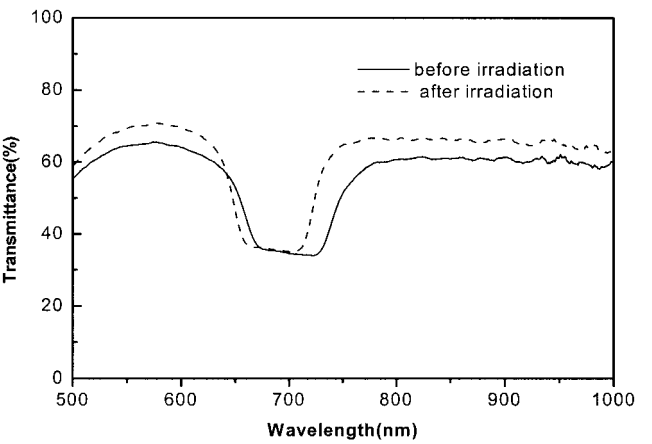

Figure 10 Dependency of reflecting spectra on UV irradiation for E48/S811/3 wt % Azo-6(a) cell.

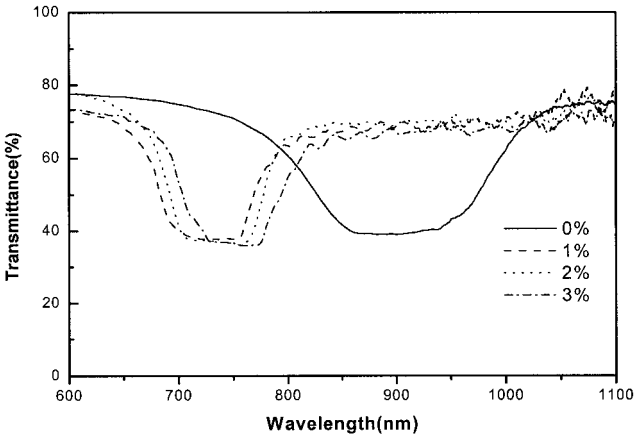

Figure 11 Effects of doping amount of azobenzene derivative 6b on reflection wavelength.

cell before and after UV irradiation. As shown in Figure 13, a repeatable and stable ON/OFF optical phenomenon was obtained. The photoisomerization of P5 film was also investigated. In theory, a laser light irradiation usually induces a *trans–cis* photoisomerization, leading to shrinkage of the films. To study the shrinkage of photoisomerization, P5 polymer was coated onto a glass surface and irradiated with an Nd-YAG 355-nm laser spot. The photoisomerization was investigated by using an atomic force microscope. As can be seen in Figure 14, a spot contraction appeared on the film surface when the film was irradiated with a laser spot. A 260 mW/cm^2 laser was used and the irradiation time was 10 s. Figure 14(a) shows the top view of the film by using SEM and Figure 14(b) shows the front view of the film by using an AFM analyzer. The diameter of the spot was about 500 nm. The spot contraction was recovered to its original even state when the film was baked at 80°C for 10 min. The result reveals the thermal isomerization of P5 film

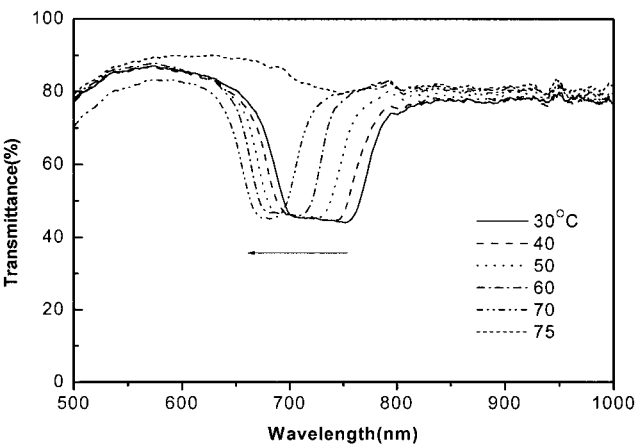

Figure 12 Dependency of reflecting spectra on temperature for E48/S811/2 wt % Azo-6(b) cell.

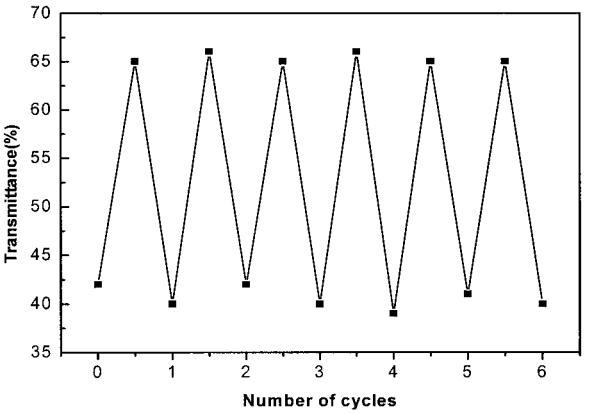

Figure 13 Reliability and stability of photoisomerization of liquid crystal cell with E48/S811/1 wt % Azo-6(a).

from *cis* to *trans* configuration. Investigation of the detailed optical properties of the chiral polymer films is now in progress.

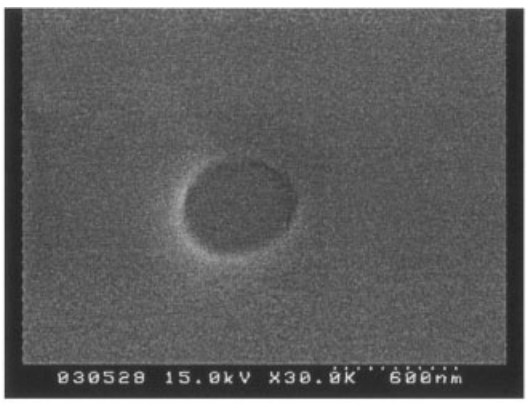

(a)

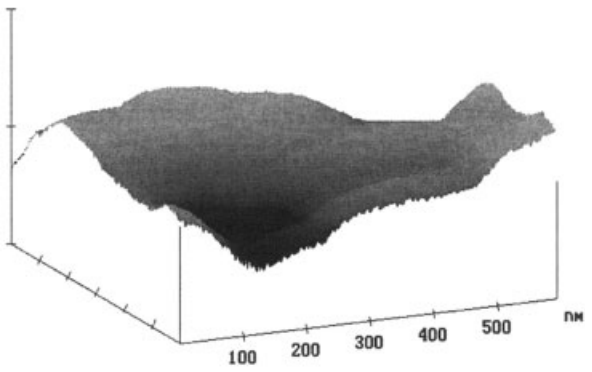

(b)

Figure 14 SEM microphotograph (a) and AFM image (b) of P5 film irradiated with Nd-YAG 355-nm laser spot.

CONCLUSIONS

A series of monomeric azobenzene derivatives of 6-(4-nitro-4′-oxy-azobenzene acrylate with carbon numbers of 6 and 11, and the chiral monomer of bornyl 4-(6-acryloyloxyhexyloxy)-phenyl-4′-benzoate were synthesized. Chiral polymers having bornyl end-capped pendants were prepared. Polymers with C_{11} spacers and alkoxyl end groups were found to have liquid crystalline properties. It was found that the response time of the *cis–trans* isomerization of the copolymers was too slow. The copolymers could not be used to fabricate the LC cells. The composite cells with chiral nematic liquid crystal and azobenzene derivatives revealed optical reflection characteristics. The optical properties of the composite cells were changed by the photoisomerization of *trans–cis* variation of azobenzene segments. The contraction of P5 film was investigated by using SEM and AFM analyzers. UV irradiation of a laser spot caused the shrinkage of the polymer film and the contraction was recovered by heat treatment.

References

1. Eich, M.; Wendorff, J. H.; Reck, B.; Ringsdorf, H. Makromol Chem Rapid Commun 1987, 8, 59.
2. Ikeda, T.; Sasaki, T.; Ichimura, K. Nature (London) 1993, 361, 428.
3. Gibbons, W. M.; Shannon, P. J.; Sun, S. T.; Swetlin, B. J. Nature (London) 1991, 351, 49.
4. Chen, A. G.; Brady, D. J. Opt Lett 1992, 17, 441.
5. Ikeda, T.; Tsutsumi, O. Science 1995, 268, 1873.
6. Tazuke, S.; Kurihara, S.; Ikeda, T. Chem Lett 1987, 911.
7. Kurihara, S.; Ikeda, T.; Sasaki, T.; Kim, H. B.; Tazuke, S. J Chem Soc Chem Commun 1990, 1751.
8. Tsutsumi, O.; Kitsunai, T.; Kanazawa, A.; Shiono, T.; Iketa, T. Macromolecules 1998, 31, 355.
9. Tsutsumi, O.; Shiono, T.; Ikeda, T.; Galli, G. J Phys Chem B 1997, 101, 1332.
10. Kanazawa, A.; Hirano, S.; Shishido, A.; Hasegawa, M.; Tsutsumi, O.; Shiono, T.; Ikeda, T.; Nagase, Y.; Akiyama, E.; Takamura, Y. Liq Cryst 1997, 23, 293.
11. Nabeshima, Y.; Shishido, A.; Kanazawa, A.; Shiono, T.; Ikeda, T.; Hiyama, T. Chem Mater 1997, 9, 1480.
12. Shishido, A.; Tsutsumi, O.; Kanazawa, A.; Shiono, T.; Ikeda, T.; Tamai, N. J Phys Chem B 1997, 101, 2806.
13. Wiesner, U.; Reynolds, N.; Boeffel, C.; Spiess, H. W. Makromol Chem Rapid Commun 1991, 12, 457.
14. Seki, T.; Sakuragi, M.; Kawanishi, Y.; Suzuku, Y.; Tamaki, T.; Fukuda, R.; Ichimura, K. Langmuir 1993, 9, 211.
15. Lee, H. K.; Kanazawa, A.; Shiono, T.; Ikeda, T.; Fijisawa, T.; Aizawa, M.; Lee, B. Chem Mater 1998, 10, 1402.
16. Kitzerow, H. Liq Cryst 1994, 16, 1.
17. Fujisawa, H.; Nakata, H.; Aizawa, M. SID Euro Display '96, 1996, 401.
18. Lovinger, A. J.; Amundson, K. L., Davis, D. D. Chem Mater 1994, 6, 1726.
19. Yamaguchi, R.; Sato, S. Jpn J Appl Phys 1992, 31, 254.
20. Yamaguchi, R.; Sato, S. Liq Cryst 1993, 14, 929.
21. Vetter, P.; Ohmura, Y.; Uchida, T. Jpn J Appl Phys 1992, 31, 1239.
22. Kajiyama, T.; Kikuchi, H.; Nakamura, K. Proc SPIE 1993, 1911, 110.
23. Liu, J. H.; Liu, H. T.; Tsai, F. R. Polym Int 1997, 42, 385
24. Liu, J. H.; Tsai, F. R.; Tsai, T. Y. Polym Adv Technol 2000, 11, 228.
25. Liu, J. H.; Wong, H. Y. J Appl Polym Sci, to appear.
26. Liu, J. H.; Shih, J. C.; Shih, C. H.; Chen, W. T. J Appl Polym Sci 2001, 81, 3538.
27. Liu, J. H.; Lin, S. H.; Shih, J. C. J Appl Polym Sci 2001, 80, 328.
28. Arima, S. Jpn. Pat., S52-13, 1985.